0026-895X/10/7801-142–150$20.00
MOLECULAR PHARMACOLOGY
Copyright © 2010 The American Society for Pharmacology and Experimental Therapeutics
Mol Pharmacol 78:142–150, 2010

Vol. 78, No. 1
63586/3600926
Printed in U.S.A.

MOL PHARM

MOLECULAR PHARMACOLOGY

The Farnesyltransferase Inhibitor LB42708 Suppresses Vascular Endothelial Growth Factor-Induced Angiogenesis by Inhibiting Ras-dependent Mitogen-Activated Protein Kinase and Phosphatidylinositol 3-Kinase/Akt Signal Pathways

Chun-Ki Kim, Yoon Kyung Choi, Hansoo Lee, Kwon-Soo Ha, Moo-Ho Won, Young-Guen Kwon, and Young-Myeong Kim

Vascular System Research Center and Department of Molecular and Cellular Biochemistry, School of Medicine (C.-K.K., Y.-K.C., K.-S.H., Y.-M.K.) and Division of Life Sciences, College of Natural Sciences (H.L.), Kangwon National University, Chuncheon, Kangwon-do, South Korea; Department of Anatomy and Neurobiology, College of Medicine, Hallym University, Chuncheon, South Korea (M.-H.W.); and Department of Biochemistry, College of Life Science and Biotechnology, Yonsei University, Seoul, South Korea (Y.-G.K.)

Received January 13, 2010; accepted April 19, 2010

ABSTRACT

Farnesyltransferase (FTase) inhibitors induce growth arrest and apoptosis in various human cancer cells by inhibiting the post-translational activation of Ras. FTase inhibitors also function to suppress the release of vascular endothelial growth factor (VEGF) from tumor cells by inhibiting Ras activation; however, the effects of FTase inhibitors on VEGF-induced angiogenesis in endothelial cells have not been studied. We have investigated the antiangiogenic effect and molecular mechanism of 4-((1-((1-((4-bromophenyl)methyl)-1*H*-imidazol-5-yl)methyl)-4-(1-napthalenyl)-1*H*-pyrrol-3-yl)carbonyl)-(9C1)-morpholine (LB42708), a selective nonpeptidic FTase inhibitor, using in vitro and in vivo assay systems. LB42708 inhibited VEGF-induced Ras activation and subsequently suppressed angiogenesis in vitro and in vivo by blocking the mitogen-activated protein kinase kinase/extracellular signal-regulated kinase/p38 mitogen-activated protein kinase (MAPK) and phosphatidylinositol 3-kinase (PI3K)/Akt/endothelial nitric-oxide synthase pathways in endothelial cells without altering FAK/Src activation. In addition, this inhibitor suppressed VEGF-induced endothelial cell cycle progression at the G_1 phase by suppressing cyclin D1 expression and retinoblastoma phosphorylation as well as up-regulating the cyclin-dependent kinase inhibitors p21 and p27. Knockdown of Ras by short interfering RNA revealed similar inhibitory effects on VEGF-induced angiogenic signal events compared with LB42708. Moreover, the inhibitory effects of LB42708 were significantly higher than those of 4-(2-(4-(8-chloro-3,10-dibromo-6,11-dihydro-5*H*-benzo-(5,6)-cyclohepta(1,2-*b*)-pyridin-11(*R*)-yl)-1-piperidinyl)-2-oxo-ethyl)-1-piperidinecarboxamide (SCH66336), a well known FTase inhibitor. LB42708 suppressed tumor growth and tumor angiogenesis in both xenograft tumor models of *Ras*-mutated HCT116 cells and its wild-type Caco-2 cells, indicating its potential application in the treatment of both *Ras*-mutated and wild type tumors. These data indicate that the antitumor effect of LB42708 can be associated with direct inhibition of VEGF-induced tumor angiogenesis by blocking Ras-dependent MAPK and PI3K/Akt signal pathways in tumor-associated endothelial cells.

Angiogenesis is the development of new blood vessels by sprouting from pre-existing endothelium of microvessels and is a significant component of a variety of pathological conditions (Folkman and Klagsbrun, 1987), including solid tumors. One of the most specific and critical regulators of angiogenesis is vascular endothelial growth factor (VEGF), which stimulates proliferation, migration, and survival through its receptors in endothelial cells (Ferrara, 2002). VEGF production is mainly up-regulated in tumor cells under hypoxic conditions and plays a pivotal role in tumor angiogenesis by activating multiple angiogenic signaling cascades for endothelial cell proliferation, migration, and differ-

This work was supported by the Korean Ministry of Education, Science, and Technology (Regional Core Research Program/Medical and Bio-Materials Research Center); and the National Research Laboratory [Grant 20090083119].
Article, publication date, and citation information can be found at http://molpharm.aspetjournals.org.
doi:10.1124/mol.110.063586.

ABBREVIATIONS: VEGF, vascular endothelial growth factor; FTase, farnesyltransferase; ERK, extracellular signal-regulated protein kinase; MAPK, mitogen-activated protein kinase; MEK, mitogen-activated protein kinase kinase; FAK, focal adhesion kinase; PI3K, phosphatidylinositol 3-kinase; eNOS, endothelial nitric-oxide synthase; NOx, nitrite plus nitrate; HUVEC, human umbilical vein endothelial cell; Rb, retinoblastoma protein; CAM, chick chorioallantoic membrane; FITC, fluorescein isothiocyanate; CDK, cyclin-dependent kinase; GGTase I, geranylgeranyltransferase I; siRNA, short interfering RNA; FBS, fetal bovine serum; PBS, phosphate-buffered saline; SCH66336, 4-(2-(4-(8-chloro-3,10-dibromo-6,11-dihydro-5*H*-benzo-(5,6)-cyclohepta(1,2-*b*)-pyridin-11(*R*)-yl)-1-piperidinyl)-2-oxo-ethyl)-1-piperidinecarboxamide; LB42708, 4-((1-((1-((4-bromophenyl)methyl)-1*H*-imidazol-5-yl)methyl)-4-(1-napthalenyl)-1*H*-pyrrol-3-yl)carbonyl)-(9C1)-morpholine.

Downloaded from molpharm.aspetjournals.org by guest on December 1, 2012

MOL PHARM
MOLECULAR PHARMACOLOGY
aspet

entiation (Ferrara, 2002; Zachary, 2003). Tumor neovascularization is essential for tumor cell proliferation and metastasis by supplying metabolic requirements for tumor growth and circulating tumor cells to spread throughout the body (Des Guetz et al., 2006). Thus, interferences with the biological activity and signal cascade of VEGF using neutralizing VEGF antibodies and its receptor tyrosine kinase inhibitors have been shown to inhibit tumor angiogenesis and prevent tumor growth and metastasis (Idbaih et al., 2008; Greenberg and Cheresh, 2009).

Ras requires farnesylation, a post-translational modification at a cysteine residue located in a distinct C-terminal motif of CAAX, for translocation to the plasma membrane leading to the formation of an active Ras-GTP complex, which is an apical signal mediator. Thus, farnesylation of Ras is an important step in the intracellular signaling pathway between receptor tyrosine kinase and cytoplasmic signaling events in cells activated by growth factors and hormones (Adjei, 2001), contributing to tumor cell proliferation and survival. Many studies have shown that inhibition of farnesyltransferase (FTase) is an attractive approach for anticancer therapy by directly inhibiting the Ras-dependent signal pathway for proliferation and survival of tumor cells (Adjei, 2001; Ravoet et al., 2008).

FTase inhibitors seem to inhibit VEGF expression and secretion from tumor cells under hypoxic conditions and by overexpression of mutant *Ras* (Rak et al., 2000; Han et al., 2005), indicating that Ras plays an important role in VEGF production in tumor cells. On the other hand, a recent study demonstrated that ectopic expression of the Ras effector mutants H-RasV12S35 or H-RasV12C40 in endothelial cells directly promotes in vitro angiogenesis by activating the ERK/MAPK and PI3K/Akt pathways (Serban et al., 2008), which are known angiogenic signal transduction pathways for endothelial cell proliferation and survival (Zachary, 2003). FTase inhibitors have been shown to inhibit in vitro endothelial cell function as well as in vivo angiogenesis in a rat corneal angiogenesis model (Gu et al., 1999; Scott et al., 2008). This evidence suggests that Ras likely involves both VEGF production in tumor cells and angiogenic signal transduction cascade in endothelial cells; however, the effect of FTase inhibitors on VEGF-induced tumor angiogenesis and its underlying molecular mechanism have not been elucidated in tumor-associated endothelial cells.

Here, we show that the new FTase inhibitor 4-((1-((1-((4-bromophenyl)methyl)-1*H*-imidazol-5-yl)methyl)-4-(1-napthalenyl)-1*H*-pyrrol-3-yl)carbonyl)-(9C1)-morpholine (LB42708) inhibits VEGF-induced angiogenesis in vitro and in vivo by blocking the MEK/ERK/p38 MAPK and Akt/eNOS/NO pathways in endothelial cells, resulting in the suppression of angiogenesis and tumor growth. Although FTase inhibitors have been generally proposed as anticancer drugs for the direct inhibition of tumor cell proliferation and survival, these results indicate that LB42708 inhibits tumor angiogenesis by blocking VEGF-induced signal pathways in tumor-associated endothelial cells.

Materials and Methods

Reagents and Antibodies. LB42708 and 4-(2-(4-(8-chloro-3,10-dibromo-6,11-dihydro-5*H*-benzo-(5,6)-cyclohepta(1,2-*b*)-pyridin-11(*R*)-yl)-1-piperidinyl)-2-oxo-ethyl)-1-piperidinecarboxamide (SCH66336, lonafarnib) were obtained from LG Life Science (Daejon, Korea) and Schering-Plough Inc. (Kenilworth, NJ), respectively. Culture media and antibiotics were purchased from Invitrogen (Carlsbad, CA), and fetal bovine serum (FBS) was obtained from HyClone Laboratories (Logan, UT). VEGF and Src antibody were purchased from Millipore (Billerica, MA). Antibodies for phosphorylated (Ser473), ERK, p38 (Thr180/Tyr182), FAK, and Src (Tyr416), as well as antibodies for Akt, ERK, and Ras, were obtained from Cell Signaling Technology (Danvers, MA). Antibodies for phospho-eNOS (Ser1177), eNOS, and phospho-tyrosine (PY20) were purchased from BD Transduction Laboratories (San Diego, CA). Antibodies for p38, FAK, and FTase α-subunit were purchased from Santa Cruz Biotechnology (Santa Cruz, CA). Transwell plate was obtained from Corning Life Sciences (Lowell, MA), and growth factor-reduced Matrigel was purchased from BD Biosciences Discovery Labware (Bedford, MA). Thermanox disc was purchased from Nalge Nunc International (Naperville, IL). All other chemicals and proteins were purchased from Sigma-Aldrich (St. Louis, MO), unless indicated otherwise.

Human Umbilical Vein Endothelial Cell Isolation and Cell Culture. Human umbilical vein endothelial cells (HUVECs) were isolated from human umbilical cord veins by collagenase treatment and grown in M119 as described previously (Lee et al., 2006) and used in passages 2 to 7. Human colorectal cancer cells (HCT116 and Caco-2) were cultured in Dulbecco's modified Eagle's medium and Eagle's minimum essential medium containing 10% FBS, 100 U/ml penicillin, and 100 μg/ml streptomycin, respectively.

In Vitro Angiogenesis Assay. Angiogenic activities of endothelial cells were determined by measurements of cell proliferation, migration, and tube formation as described previously (Namkoong et al., 2005; Lee et al., 2006). Cell proliferation was determined by [^{3}H]thymidine incorporation assay. Cells pretreated with FTase inhibitors were stimulated by the addition of VEGF (10 ng/ml) for 24 h followed by the addition of 0.5 μCi/ml [^{3}H]thymidine for 6 h. ^{3}H-Labeled radioactive material was precipitated using 10% trichloroacetic acid at 4°C for 30 min. After washing twice with ice-cold H_2O, ^{3}H-labeled radioactive material was solubilized in 0.2 N NaOH containing 0.1% SDS. ^{3}H-Labeled radioactivity was determined by a liquid scintillation counter. Migration assay was performed using Transwell plates with 6.5-mm diameter polycarbonate filters (8 μm pore size). The lower surface of the filter was coated with 10 μg of gelatin. Fresh M199 media (1% FBS) containing VEGF was placed in the lower wells. HUVECs pretreated with FTase inhibitors were trypsinized and suspended at a final concentration of 10^6 cells/ml in M199 containing 1% FBS. One hundred microliters of the cell suspension was loaded into each of the upper wells. After incubation at 37°C for 4 h, cells were fixed and stained with hematoxylin and eosin. Chemotaxis was quantified by counting the cells that migrated to the lower side of the filter at low power fields (100×) using a phase-contrast microscope. Tube formation was determined after culturing HUVECs on a layer of growth factor-reduced Matrigel. Twenty-four-well culture plates were coated with Matrigel according to the manufacturer's instructions. HUVECs pretreated with FTase inhibitors were plated onto a layer of Matrigel at a density of 2.0×10^5 cells/well followed by the addition of VEGF. Matrigel cultures were incubated at 37°C for 20 h. Tube formation was observed using an inverted phase-contrast microscope. The degree of tube formation was quantified using the Image-Pro Plus version 4.5 (Media Cybernetics, San Diego, CA).

Ex Vitro and In Vivo Angiogenesis Assay. For aortic ring sprouting assay, rat aortas were transversely cut by 1-mm thickness after harvesting from 6-week-old male Sprague-Dawley rats (Orient, Sungnam, Korea) and placed in the 48-well plates coated with 100 μl of Matrigel. FTase inhibitors (200 nM) and/or VEGF (20 ng/ml) was added to the wells at a final volume of 200 μl of human endothelial serum-free medium. On day 6, microvessel outgrowth was photographed under a phase-contrast microscope (Lee et al., 2006). Chick chorioallantoic membrane (CAM) assay was carried out as described previously (Lee et al., 2006). In brief, Thermanox discs containing 5

Downloaded from molpharm.aspetjournals.org by guest on December 1, 2012

MOL PHARM
MOLECULAR PHARMACOLOGY
aspet

μl of salt-free solution containing FTase inhibitor (200 nM) with or without 5 μl of VEGF (10 μg/ml) were loaded onto the CAM of 10-day-old embryos. After 70-h incubation at 37°C, the area around the loaded disc was photographed with a digital camera. Neovascularization was determined by intravital fluorescence microscopy as described previously (Lee et al., 2006; Namkoong et al., 2008). Matrigel (100 μl) containing VEGF (100 ng) alone or plus LB42708 (1 μmol) was injected into the inner space of window, which was surgically implanted between the skin and abdominal wall of male BALB/c mice (6–8 weeks old). After 4 days, neovascularization was recorded by a Zeiss Axiovert 200M microscope (Carl Zeiss, Inc., Thornwood, NY) after intravenous injection of 50 μl of 25 mg/ml FITC-labeled dextran (molecular weight, 250,000) via the tail vein. The relative angiogenic activity was scored from 0 (least positive) to 5 (most positive) in a double-blinded manner.

Western Blot Analysis and Nitric Oxide Assay. Lysates of HUVECs were separated by SDS-polyacrylamide gel electrophoresis, and the levels of target proteins were determined by Western blot analysis (Lee et al., 2006). The intracellular NO level in HUVECs was measured in situ using 4-amino-5-methylamino-2′,7′-difluorescein diacetate (Invitrogen, Carlsbad, CA) using a confocal laser microscope (Lee et al., 2006). The levels of nitrite plus nitrate (NOx) were determined in the culture medium by a chemiluminescent NO analyzer (Antek, Houston, TX).

Ras Activation Assay. The activation of Ras was evaluated using a Ras Activation Assay kit according to the manufacturer's protocol (Millipore). In brief, cell lysates (400 μg of protein) were incubated with 5 μg of Raf-1 Ras binding domain-conjugated agarose for 45 min at 4°C. The agarose beads were collected by centrifugation at 12,000*g* for 5 s and washed three times with lysis buffer. The pellets were suspended with 2× sample buffer and separated by 15% SDS-polyacrylamide gel electrophoresis. Ras protein level was determined by Western blotting using a pan-Ras antibody.

Cell Cycle Analysis. HUVECs were pretreated with FTase inhibitors (100 nM) or transfected with siRNA (40 nM) in M199 containing 10% FBS for 12 h. For synchronization in G_1/S boundary, cells were cultured in M119 containing 1% FBS plus 5 mM thymidine for 12 h, followed by stimulation with VEGF (10 ng/ml) for 18 h. The cells were collected by trypsinization, washed with phosphate-buffered saline (PBS), and fixed in 70% ethanol for 30 min at 4°C. After washing with PBS, cells were incubated with 500 μl of propidium iodide staining solution (50 μg/ml propidium iodide, 10 μg/ml RNase, and 0.1% Nonidet P-40 in PBS) for 30 min at 37°C in the dark. Cell cycle was determined using a flow cytometer and cell fit software (BD Biosciences, San Jose, CA).

Mouse Xenograft Experiments. Female nude mice (6–7 weeks old; Charles River Laboratories Inc., Wilmington, MA) were subcutaneously inoculated with 10^7 cells of the human colon carcinoma cells HCT116 and Caco-2, and treatment was initiated after ~7 days when tumor volumes uniformly reached 60 to 80 mm^3. Mice were then intraperitoneally injected with LB42708 (20 mg/kg/day) or vehicle control (0.1% dimethyl sulfoxide in 0.9% saline). Tumors were measured twice weekly with a digital caliper, and their volumes were calculated according to the formula length × width × height × 0.5236. After 35 days of tumor cell inoculation, tumors were harvested by resection, and their weight was measured.

Immunohistochemistry. Tumor sections were incubated in 0.3% hydrogen peroxide in methanol for 15 min to block endogenous peroxidase, washed three times with PBS, blocked for 2 h at room temperature with 3% normal goat in PBS, and finally incubated overnight at 4°C with primary antibody against human CD31. Sections were washed three times with PBS and incubated with a secondary antibody conjugated with tetramethylrhodamine isothiocyanate for a CD31 antibody for 1 h. After washing three times with PBS and incubated with FITC-labeled isolectin B_4 (5 μg/ml; Vector Laboratories, Burlingame, CA) for 30 min. The sections were mounted with Permount solution after washing three times with PBS. Tumor vessels were photographed using a fluorescence microscope, and vessel density was quantified using the software Image-Pro Plus (Media Cybernetics, Bethesda, MD).

Transfection with siRNA. Oligonucleotide sequences of *Ras*-specific siRNAs were 5′-AATAGAGGATTCCTACAGGAA-3′ for H-/K-Ras and 5′-AAGTCTTTTGAGGACATCCAC-3′ for H-Ras. FTase α-subunit siRNA was purchased from Santa Cruz Biotechnology. The sequence of scramble siRNA was 5′-CAGTCGCGTTTGCGACTGGTT-3′. The siRNAs were synthesized with the Silencer siRNA Construction Kit according to the manufacturer's protocol (Ambion, Austin, TX). All siRNAs (mixture of 20 nM H-/K-Ras and 20 nM H-Ras or 40 nM scramble siRNA) were transfected into cells using a MicroPorator (NanoEnTek, Seoul, Korea). The transfected cells were cultured in complete media without antibiotics for 12 h and further cultured in complete media for 12 h.

Statistic Analysis. The data are presented as the mean ± S.D. of at least three separate experiments. Comparisons between two groups were analyzed using Student's *t* test, and significance was established at $P < 0.05$.

Results

LB42708 Inhibits VEGF-Induced Angiogenesis In Vitro. We first examined the in vitro effect of the FTase inhibitor LB42708 on VEGF-induced endothelial cell proliferation. Treatment of HUVECs with LB42708 resulted in an inhibition of VEGF-induced DNA synthesis in a dose-dependent manner up to 100 nM, with an IC_{50} value of approximately 75 nM (Fig. 1A). We next determined whether LB42708 regulates endothelial cell migration in a Transwell assay system. Treatment with LB42708 inhibited VEGF-induced chemotactic motility of HUVECs, whereas this com-

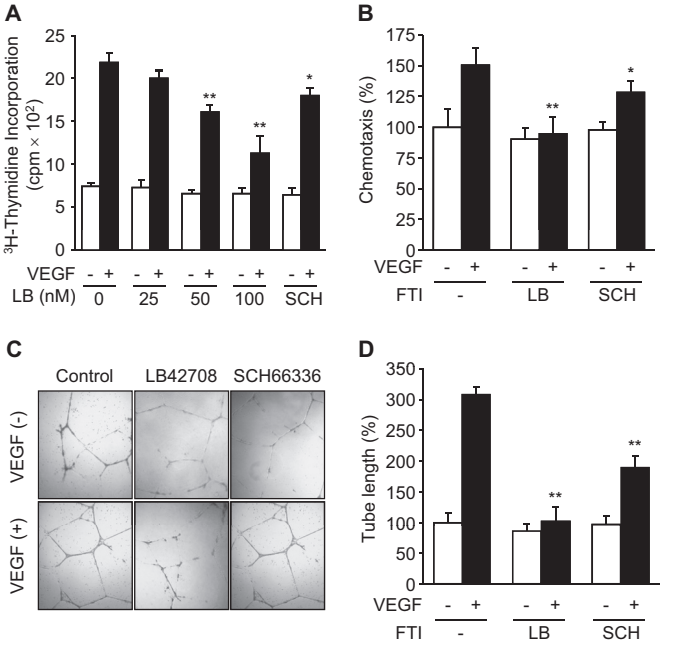

Fig. 1. LB42708 inhibits VEGF-induced in vitro angiogenesis. HUVECs were pretreated with or without the indicated concentrations or 100 nM LB42708 (LB) or 100 nM SCH66336 (SCH) for 24 h. A, cells were stimulated with VEGF (10 ng/ml) for 30 h and incubated with 1 μCi/ml [^{3}H]thymidine for 6 h. Cell proliferation was determined by [^{3}H]thymidine incorporation assay. B, cells were stimulated with VEGF (10 ng/ml) in Transwell plates for 4 h, and cell migration was determined in Transwell plates by counting the migrated cells. C and D, cells were cultured on a layer of Matrigel with VEGF (10 ng/ml) for 24 h. Tube formation was observed using an inverted phase-contrast microscope with a video graphic system. All graphic data are the mean ± S.D. ($n = 4$). *, $P < 0.05$, and **, $P < 0.01$ versus VEGF alone.

Downloaded from molpharm.aspetjournals.org by guest on December 1, 2012

MOL PHARM
MOLECULAR PHARMACOLOGY
aspet

pound did not alter basal migration of endothelial cells devoid of VEGF stimulation (Fig. 1B). We further examined the effect of LB42708 on tube-like structure formation of endothelial cells on Matrigel-coated plates. LB42708 treatment effectively suppressed VEGF-induced increases in the formation of elongated and strong tube-like structures, whereas it had no significant effect on tube formation of control endothelial cells (Fig. 1, C and D). When the inhibitor was removed during incubation with VEGF, its inhibitory effect on tube formation was not observed, but in part was reversed (data not shown), suggesting that farnesylation of Ras is a rate-limiting step in VEGF-induced angiogenesis. No cytotoxic effect was observed in HUVECs exposed directly to LB42708 up to 10 μM for 48 h (data not shown), indicating that the in vivo antiangiogenic effect of LB42708 is not due to cytotoxicity. It is noteworthy that the inhibitory effects of LB42708 on VEGF-induced angiogenic events were significantly greater than those of the well characterized FTase inhibitor SCH66336, which is currently being evaluated in clinical trials (Ravoet et al., 2008), at 100 nM (Fig. 1, A–D). These results suggest that LB42708 has the ability to inhibit VEGF-induced in vitro angiogenesis and possesses higher antiangiogenic activity than SCH66336.

LB42708 Inhibits VEGF-Induced Angiogenesis Ex Vivo and In Vivo. We next determined the ex vivo effect of LB42708 on vessel sprouting from aortic rings placed in Matrigel containing VEGF. LB42708 significantly inhibited vessel sprouting in the cut edge of rat aortic rings exposed to VEGF and in part suppressed basal sprouting activity of control aortic rings, and this inhibitory effect was significantly greater than that of SCH66336 (Fig. 2, A and B). We next investigated whether LB42708 is capable of regulating in vivo angiogenesis using the CAM assay. VEGF markedly increased the total surface density of capillaries compared with untreated control, and this increase was reduced to a level similar to that of control, by cotreatment with LB42708 (Fig. 2, C and D). Treatment with LB42708 alone revealed partial inhibition of basal angiogenesis but did not show an inhibitory effect on pre-existing larger vessels or signs of toxicity, such as thrombosis and hemorrhage (Fig. 2, C and D). We further confirmed the antiangiogenic capability of LB42708 in an animal model by intravital microscopy. VEGF increased angiogenic characteristics, such as capillary sprouting and bud formation, which were significantly inhibited by cotreatment with LB42708. Moreover, treatment with this inhibitor alone showed partial suppression of basal neovessel formation (Fig. 2, E and F). These results indicate that LB42708 is capable of inhibiting VEGF-induced neovessel formation in vivo.

LB42708 Inhibits VEGF-Induced Activation of MAPKs, Akt, and eNOS but Not Src and FAK. We examined whether FTase inhibitor regulates VEGF receptor KDR/Flk-1 phosphorylation, which is the initial step in VEGF-induced angiogenic signaling (Ferrara, 2002). Neither LB42708 nor SCH66336 inhibited KDR phosphorylation in VEGF-stimulated HUVECs up to 100 nM (Fig. 3A), indicating that these FTase inhibitors do not interfere with KDR activity. KDR/Flk-1 exhibits intrinsic protein tyrosine kinase activity, which may be involved in Ras activation and the subsequent generation of its GTP-bound form, resulting in the formation of the active Raf-1/Ras-GTP complex (Guo et al., 1995; Schubbert et al., 2007). To examine the effect of LB42708 on VEGF-induced Ras activation, HUVECs pretreated with LB42708 were exposed to VEGF and then examined for Ras activation by immunoprecipitation of Ras-GTP. LB42708 inhibited VEGF-induced formation of the GTP-bound form of Ras in a dose-dependent manner, with an IC_{50} value of approximately 50 nM, and its inhibitory activity was significantly greater than that of SCH66336 (Fig. 3B). We next examined the effect of LB42708 on VEGF-induced phosphorylation of Src and FAK, which are downstream mediators of KDR/Flk-1 autophosphorylation (Zachary, 2003). Neither FTase inhibitor inhibited VEGF-induced phosphorylation of FAK and Src up to 100 nM (Fig. 3, C and D). Because the MAPK and PI3K/Akt/eNOS pathways have been demonstrated to be critically involved in VEGF-induced angiogenesis (Ferrara, 2002; Zachary, 2003; Lee et al., 2006), the effects of LB42708 on VEGF-induced MAPK, Akt, and eNOS activation were examined. LB42708 inhibited the phosphorylation of ERK and p38 MAPK in VEGF-stimulated HUVECs in a dose-dependent manner (Fig. 3, E and F). In addition, this inhibitor decreased VEGF-induced Akt and eNOS activation (Fig. 3, G and H). Phosphorylation-dependent activation of eNOS increases NO production, which plays a key role in VEGF-stimulated angiogenesis (Lee et al., 2006). LB42708 inhibited VEGF-induced increases in intracellular NO production and accumulation of NOx in culture medium (Fig. 3, I and J). NOx accumulation was revealed to be the result of

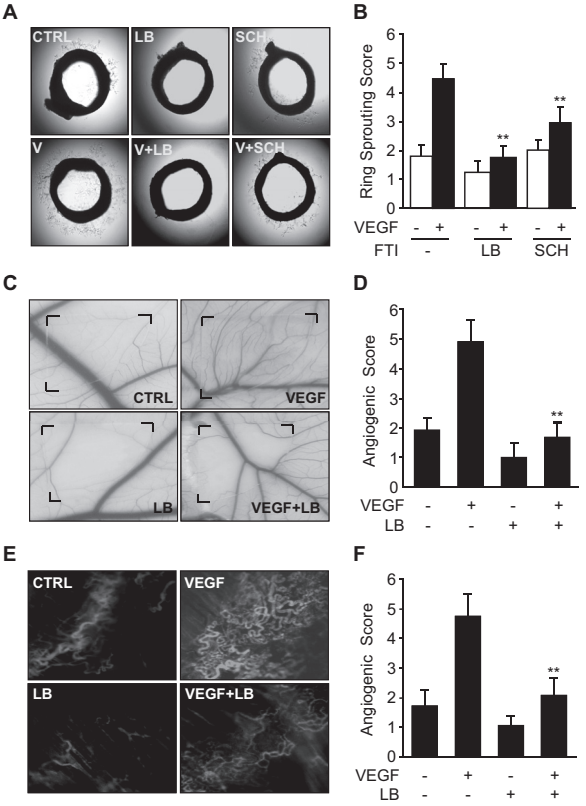

Fig. 2. LB42708 inhibits VEGF-induced angiogenesis ex vivo and in vitro. A and B, rat aortic rings were cultured with FTase inhibitors (200 nM) and/or VEGF (20 ng/ml) in 48-well plates coated with 100 μl of Matrigel. On day 6, microvessel outgrowth was determined using a phase-contrast microscope. C and D, FTase inhibitors (200 nM/5 μl) and/or VEGF (10 ng/5 μl) were loaded onto the CAMs of day 10 chick embryos. After 72-h incubation, discs and surrounding CAMs were photographed. E and F, Matrigel (100 μl) containing LB42708 (1 μmol) and/or VEGF (100 ng) was put into the abdominal windows of mice. After 4 days, neovascularization was recorded by intravital fluorescence microscopy. Relative angiogenic activities were scored from 0 (least positive) to 5 (most positive). Data shown are the mean ± S.D. ($n \geq 7$). **, $P < 0.01$ versus VEGF alone.

Downloaded from molpharm.aspetjournals.org by guest on December 1, 2012

MOL PHARM

MOLECULAR PHARMACOLOGY

eNOS activation, because administration of the eNOS inhibitor N^G-monomethyl L-arginine blocked NO production (Fig. 3J). Moreover, the inhibitory effects of LB42708 were higher than those of SCH66336 at 100 nM (Fig. 3, E–H, J). These results suggest that LB42708 inhibits VEGF-induced angiogenesis by blocking Ras-dependent activation of ERK, p38 MAPK, Akt, and eNOS without inhibiting the FAK and Src pathways.

Knockdown of FTase and Ras Inhibits VEGF-Induced Signal Pathways and Angiogenic Events. To investigate the involvement of FTase and Ras in VEGF-mediated signal pathways and angiogenesis, we used siRNA approaches to selectively knock down the FTase α-subunit and Ras. Protein levels of the FTase α-subunit and Ras were specifically knocked down in HUVECs by transfection with siRNAs but not with scrambled siRNA (Fig. 4A). We next examined whether the FTase α-subunit and Ras regulates VEGF-induced angiogenic signaling events. As expected, transfection with FTase α-subunit-specific siRNA inhibited VEGF-induced activation of ERK and Akt but not FAK and Src (Fig. 4B). In addition, transfection with Ras-specific siRNA inhibited VEGF-induced activation of ERK, p38 MAPK, Akt, and eNOS, whereas these suppressive effects were not observed in scrambled siRNA-transfected HUVECs (Fig. 4C). VEGF-induced activation of FAK and Src was not affected by transfection with Ras siRNA (Fig. 4C). Furthermore, VEGF-induced increases in HUVEC proliferation and migration were effectively diminished by transfection with Ras-specific siRNA but not by scrambled siRNA (Fig. 4, D and E). These results suggest that FTase-dependent Ras activation is critically involved in VEGF-elicited angiogenic signal transduction and angiogenesis.

LB42708 and Ras-Specific Knockdown Block VEGF-Induced Endothelial Cell Cycle Progression by Arresting Cells at the G_1 Phase. Ras plays an important role in cell cycle progression via the regulation of cyclin expression (Pruitt and Der, 2001). We examined the effects of LB42708 and Ras-knockdown on cell cycle progression using fluorescence-activated cell sorting analysis. VEGF induced HUVECs into S phase from G_1 phase of the cell cycle, whereas treatment with LB42708 and Ras-specific siRNA, but not scrambled siRNA, markedly reduced S-phase entry elicited by VEGF (Fig. 5A). Because cell cycle progression is regulated by expression levels of cyclins, we examined whether LB42708 and Ras knockdown regulated protein levels of cyclins. VEGF elevated the protein levels of cyclins D1, E, A, and B, and these increases were inhibited by treatment with LB42708 and transfection with Ras-specific siRNA but not by scrambled siRNA (Fig. 5B). Furthermore, LB42708 revealed stronger effects on cell cycle arrest and cyclin expression than SCH66336 (Fig. 5, A and B). The cell cycle transition from G_1 phase to S phase is primarily regulated by up-regulation of cyclin D1 expression. Cyclin D1 is known to regulate the activity of cyclin-dependent kinase 4 (CDK4), which phosphorylates the retinoblastoma (Rb) protein (Sherr, 1995). Therefore, we next examined the phosphorylation state of Rb in endothelial cells. LB42708 and Ras siRNA-mediated knockdown inhibited the hyperphosphorylation of Rb induced by VEGF at serine residues 780, 795, and 807/811 (Fig. 5C). In addition, we examined the effect of LB42708 and Ras siRNA on protein levels of the cell cycle regulators, p53, p21, and p27, which arrest cell cycle at the G_1 phase. LB42708 and Ras siRNA, but not scrambled siRNA, blocked VEGF-induced decreases in expression levels of p53, p21, and p27 (Fig. 5D). These results indicate that LB42708 inhibits endothelial cell proliferation via the arrest of the cell cycle at G_1 phase by suppressing cyclin D1 expression and Rb phosphorylation as well as elevating protein levels of cell cycle inhibitors.

LB42708 Reduces Tumor Growth and Angiogenesis in Human Tumor Xenograft Models. To evaluate the effect of LB42708 on tumor growth and angiogenesis, we used a human colon cancer xenograft mouse model. After tumor formation (60–80 mm^3) in mice subcutaneously in-

Downloaded from molpharm.aspetjournals.org by guest on December 1, 2012

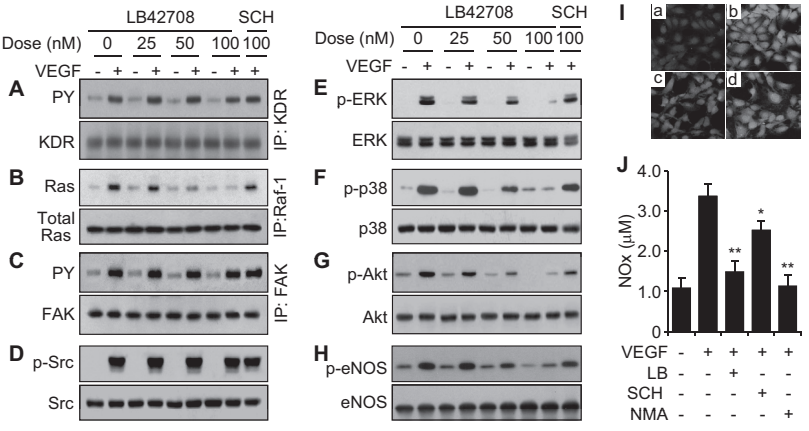

Fig. 3. LB42708 regulates the VEGF-induced angiogenic signaling pathway. HUVECs were pretreated with the indicated concentrations or 100 nM FTase inhibitors for 24 h and then stimulated with or without VEGF (10 ng/ml) in the presence of the same concentrations of pretreated FTase inhibitors for 10 min (A–F) or 30 min (G and H). A and C, cell lysates (400 μg of protein) were incubated with antibodies (25 μg) against KDR and FAK overnight and then treated with agarose-A/G for 4 h. B, cell lysates (400 μg of protein) were incubated with agarose-conjugated Raf-1 Ras binding domain (5 μg) for 45 min. A to C, after centrifugation at 12,000*g* for 5 s, Western blot was performed with antibodies for target proteins and phosphotyrosine (PY). D to H, lysates were separated on SDS-polyacrylamide gel electrophoresis, and targets proteins were determined by Western blotting. I, after stimulation with 10 ng/ml VEGF for 1 h, cells were incubated with the NO-specific probe 4-amino-5-methylamino-2′,7′-difluorescein diacetate (5 μM) for 1 h. Intracellular levels of NO were determined by confocal microscopy. a, control; b, VEGF; c, VEGF + LB42708; d, VEGF + SCH66336. J, the levels of NOx were measured in culture media from cells treated with VEGF (10 ng/ml) for 24 h using an NO analyzer. N^G-Monomethyl L-arginine (1.5 mM) was also added to the culture media during stimulation with VEGF. Data shown are the mean ± S.D. (n = 3). *, $P < 0.05$ and **, $P < 0.01$ versus VEGF alone.

jected with *Ras*-mutated HCT116 and wild-type Caco-2 cells, mice were intraperitoneally injected with or without LB42708, and tumor sizes were measured twice weekly for 35 days. LB42708 administration significantly inhibited the growth of both tumors (Fig. 6, A and B) and microvessel formation surrounding tumors (Fig. 6, C and D). At day 35, the tumors were removed, and their size and weight were measured. Tumor weights in control groups of Caco-2 and HCT116 tumors were 0.62 ± 0.09 and 0.81 ± 0.12 g, respectively, whereas LB42708 treatment reduced their weights to 0.31 ± 0.08 and 0.15 ± 0.06 g (n = 7; data not shown). Thus, LB42708 treatment reduced tumor weight by 51 and 80% for Caco-2 and HCT116 tumors, respectively, compared with each control. These data indicate that the therapeutic effect of LB42708 is greater for *Ras*-mutated HCT116 tumors than for wild-type Caco-2 tumors. We next examined the effect of LB42708 on angiogenesis in both tumors by immunohistochemistry. The density and size of vessels were higher and larger in HCT116 tumors than in Caco-2 tumors, and vessel density in both tumors was significantly decreased by treatment with LB42708 (Fig. 6, E and F). These results together suggest that LB42708 inhibits tumor growth and angiogenesis in both *Ras* wild-type and mutated tumors.

Discussion

The oncogene *Ras* gene family consists of three functional genes, H-*Ras,* N-*Ras,* and K-*Ras*, which are involved in the receptor tyrosine kinase-mediated signal pathways critical for tumor growth and survival. Mutated Ras that remains in its active state longer than wild-type Ras exists in 20 to 30% of all cancers (Rodenhuis, 1992). Because farnesylation of Ras is the first and rate-limiting step for its membrane localization and subsequent activation, FTase inhibitors have been demonstrated to directly abrogate tumor promotion and growth. Therefore, FTase inhibitors are a very attractive target for anti-tumor drugs through the direct inhibition of tumor cell function (Head and Johnston, 2004). Results presented herein demonstrate that the new FTase inhibitor LB42708 directly inhibits VEGF-induced signal pathway and angiogenesis in vitro and in vivo, which is closely associated with tumor growth in human tumor xenograft models of *Ras*-mutated HCT116 and wild-type Caco-2 cells. These data indicate that LB42708 can inhibit tumor growth via suppression of tumor angiogenesis by directly targeting tumor-associated endothelial cells.

Angiogenesis is crucial for the pathogenesis or progression of human diseases, particularly solid tumors. Solid tumors produce VEGF, which promotes tumor angiogenesis, leading to tumor growth and metastasis (Des Guetz et al., 2006;

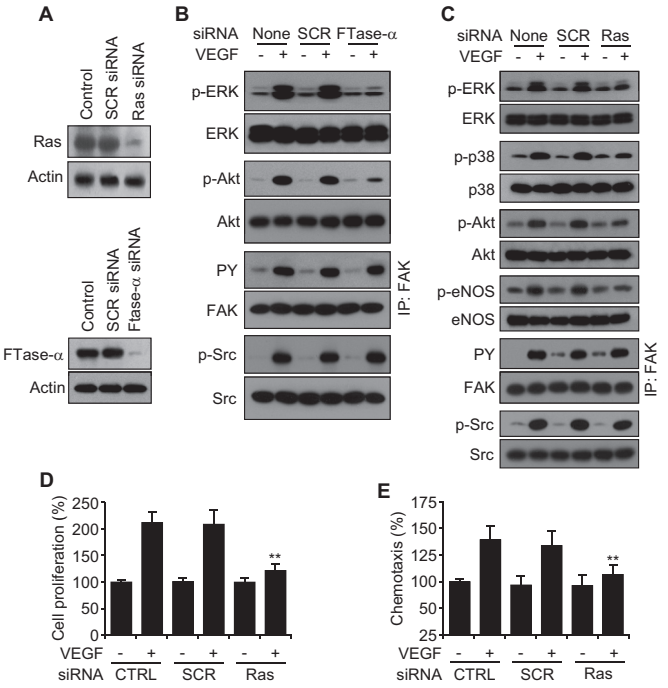

Fig. 4. Specific knockdown of FTase and Ras inhibits VEGF-induced signal transduction and in vitro angiogenesis. A, HUVECs were transfected with 40 nM siRNA specific for the FTase α-subunit and Ras using a MicroPorator. After recovery of cells for 24 h, the protein levels of FTase α-subunit and Ras were determined by Western blotting. B and C, cells transfected with siRNA specific for the FTase α-subunit and Ras were treated with VEGF (10 ng/ml) for 10 min (ERK and p38) or 30 min (other proteins). The levels of phosphorylated proteins were determined by Western blotting analysis using antibodies for target proteins and phosphotyrosine (PY). Cell proliferation (D) and migration (E) were determined in siRNA-transfected cells by [^{3}H]thymidine incorporation assay and using Transwell plates, respectively, as described in Fig. 1. Data shown are the mean ± S.D. (n = 3). **, $P < 0.01$ versus VEGF in scrambled siRNA-transfected cells.

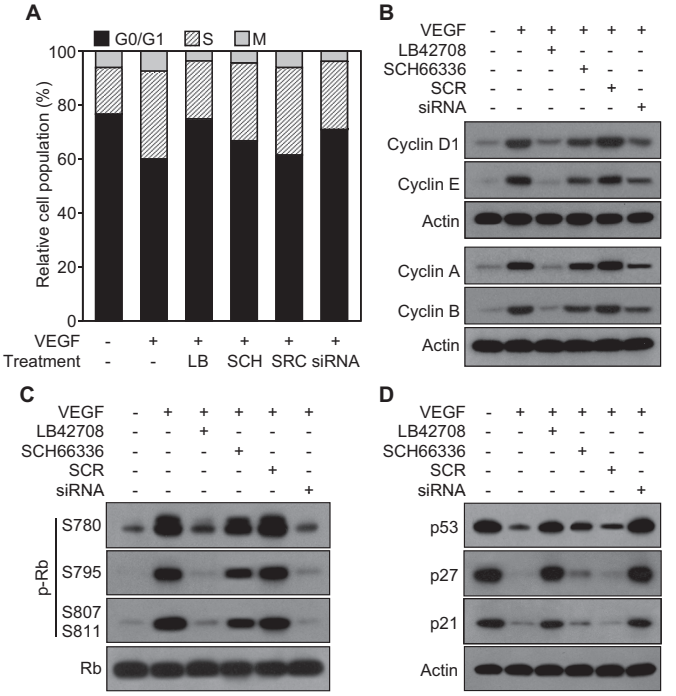

Fig. 5. LB42708 and Ras knockdown blocks VEGF-induced endothelial cell cycle progression by arresting cells at the G_1 phase. A, HUVECs were pretreated with FTase inhibitors (100 nM) or transfected with siRNA (40 nM) for 24 h and further incubated with 5 mM thymidine in M119 containing 1% FBS for 12 h. Cells were stimulated with VEGF (10 ng/ml) in M119 containing 1% FBS for 18 h. Cell cycle was analyzed by fluorescence-activated cell sorting. Data shown are average values (n = 2). B, HUVECs pretreated with FTase inhibitors (100 nM) or transfected with siRNA (40 nM) were cultured in M119 containing 1% FBS for 6 h. Cells were incubated with 10 ng/ml VEGF for 8 and 12 h to determine the levels of cyclins D1 and E and cyclins A and B, respectively. The levels of cyclins were determined by Western blot analysis. After incubation with VEGF for 8 h, the levels of p-Rb (C) and cell cycle regulators such as p53, p21, and p27 (D) were determined by Western blot analysis.

MOL PHARM
MOLECULAR PHARMACOLOGY
aspet
Downloaded from molpharm.aspetjournals.org by guest on December 1, 2012

Greenberg and Cheresh, 2009). Therefore, therapies using anti-VEGF antibodies and VEGF-mediated signal blockers inhibit tumor growth and metastasis, leading to the improvement of cancer patient survival by blockade of tumor angiogenesis (Idbaih et al., 2008; Greenberg and Cheresh, 2009). These studies emphasize that VEGF is a major tumor angiogenic factor and plays an important role in the development and progression of solid tumors. The first generation of the nonpeptide pyrole-based FTase, LB42908, inhibited FTase activities toward recombinant H-Ras and N-Ras with IC_{50} values of 0.9 and 2.4 nM, respectively (Lee et al., 2001), and its advanced compound LB42708 used in this study was a more potent inhibitor in vitro and in vivo (Na et al., 2004; Kim et al., 2006). The inhibitory activity of LB42708 was higher than that of SCH66336, which blocked farnesylation of H-Ras and N-Ras with IC_{50} values of 1.9 and 2.8 nM, respectively (Liu et al., 1998). Both inhibitors showed comparable inhibitory activities on the related geranylgeranyltransferase I (GGTase I) at concentrations as high as 50 μM (Liu et al., 1998; Lee et al., 2001). These observations indicate that LB42708 is a more selective inhibitor of FTase (>50,000-fold) over GGTase I than SCH66336 (>25,000-fold). Our previous study demonstrated that LB42708 is a more potent inhibitor for post-translational modification of Ras (IC_{50} = 10 nM) and inflammatory gene expression than SCH66336 (IC_{50} = ~50 nM) in immune-activated RAW264.7 cells (Na et al., 2004). These observations suggest that LB42708 elicits a greater inhibitory effect on Ras activation than SCH66336. Indeed, we found here that LB42708 significantly inhibited VEGF-induced formation of an active Ras-GTP complex in primary cultured HUVECs, with an IC_{50} of ~50 nM; however, SCH66336 slightly inhibited Ras activation at 100 nM in cultured endothelial cells (Fig. 3B). These values were significantly higher than IC_{50} values calculated in an in vitro incubation system of FTase, Ras protein, and farnesylpyrophosphate. This discrepancy may be due to their biological activities and chemical properties, such as selectivity for FTase over GGTase I, membrane permeability, and solubility. We also found that the inhibitory effects of LB42708 on VEGF-induced angiogenic signal transduction were stronger than that of SCH66336. Although FTase inhibitors can suppress angiogenesis by blocking VEGF production from tumor cells (Rak et al., 2000; Han et al., 2005), our results showed that LB42708 inhibited VEGF-induced angiogenic signaling pathways and subsequently blocked angiogenesis in vitro and in vivo. We also found that FTase inhibits VEGF expression and production from hypoxic tumors (data not shown), and the detailed regulating mechanism for the suppressive effect of FTase inhibitor on VEGF expression in tumors is now under investigation. Our results suggest that the suppression of tumor angiogenesis by LB42708 is associated with dual mechanisms, such as the inhibition of VEGF expression from tumors (Rak et al., 2000; Han et al., 2005) and the suppression of tumor angiogenesis by interfering with the Ras-dependent angiogenic signaling pathways triggered by VEGF produced from both *Ras*-mutated and wild-type tumors.

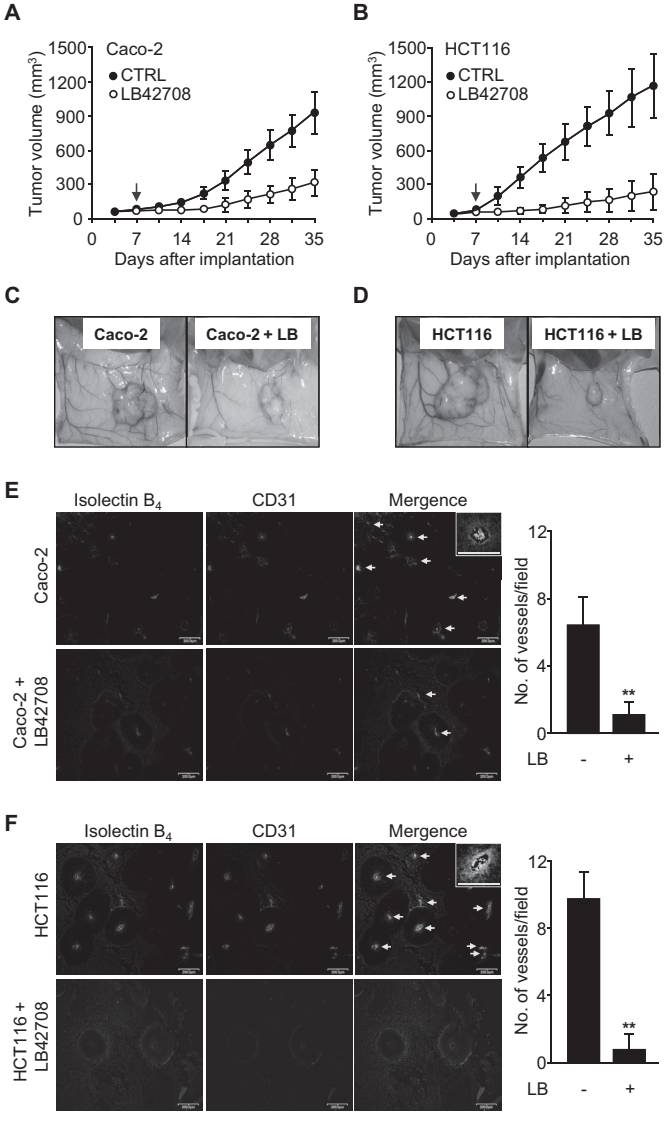

Fig. 6. LB42708 reduces tumor growth and angiogenesis in human tumor xenograft models. Human colon cancer Caco-2 cells and HCT116 cells were implanted into the right flank of nude mice. From 7 days after implantation, mice were injected daily with LB42708 (20 mg/kg i.p.) or vehicle control (0.1% dimethyl sulfoxide in 0.9% saline). A and B, tumor volumes were monitored twice weekly for 35 days. Data shown are the mean ± S.D. (n = 6). C and D, at day 35, the mice were sacrificed, and tumors and surrounding vasculature were photographed. E and F, tumor vessels were determined by immunohistochemistry using an FITC-labeled isolectin B_4 and an anti-CD31 antibody. Vessel density was quantified using the software Image-Pro Plus. Data shown are the mean ± S.D. (n = 4). **, $P < 0.01$ versus control.

VEGF promotes angiogenesis through the activation of multiple signal transduction pathways, such as Src/FAK, MAPKs, Akt/eNOS, and NO production, through the activation of its receptor-2 KDR//Flk-1 (Zachary, 2003). The ERK and p38 MAPK pathways are a requisite for the proliferative and migrating activities of VEGF in endothelial cells, and the Akt/eNOS/NO pathway is responsible for VEGF-induced endothelial survival and proliferation (Zachary, 2003; Lee et al., 2006). However, activation of Src and FAK is also important for endothelial cell migration in response to VEGF (Zachary, 2003). The angiogenic signal mediators ERK and p38 MAPK are known to be activated via the Raf-1/MEK pathway, and Akt phosphorylation is directly dependent on PI3K activation. Both signal pathways are downstream of Ras activation (Schubbert et al., 2007). Our data showed that LB42908 and Ras knockdown effectively inhibited the VEGF-induced classic angiogenic signaling pathways, such as ERK and p38 MAPK activation and the Akt/eNOS/NO pathway, but not

MOL PHARM
MOLECULAR PHARMACOLOGY
aspet
Downloaded from molpharm.aspetjournals.org by guest on December 1, 2012

MOL PHARM
MOLECULAR PHARMACOLOGY

VEGF-induced Src and FAK activation. Furthermore, transfection with siRNA specific for the active FTase α-subunit and Ras inhibited VEGF-induced activation of ERK and Akt but not Src and FAK. In addition, LB42908 inhibited VEGF-induced formation of the Ras-GTP complex, which is the active form of Ras. These results suggest that LB42908 effectively inhibited VEGF-induced Ras activation, which plays a role of a signal linker between KDR//Flk-1 and Raf-1/MEK/ERK/p38 MAPK and PI3K/Akt/eNOS in the VEGF-induced angiogenic signaling pathways (Fig. 7). However, activation of Src and FAK by VEGF is not associated with the Ras-dependent pathway.

Cell proliferation is closely associated with cell cycle progression, and chemicals that inhibit cell cycle progression are able to block endothelial cell proliferation, resulting in the suppression of angiogenesis (Hanai et al., 2002; Min et al., 2004). The well known antiangiogenic molecule endostatin inhibits endothelial cell proliferation through cell cycle arrest at the G_1 phase by suppressing cyclin D1 expression and Rb phosphorylation (Hanai et al., 2002). The cyclin D1 regulates the activity of CDK4, which phosphorylates Rb. Phosphorylated Rb releases E2F to activate genes whose functions are required for S-phase entry, in turn leading to DNA synthesis and cell cycle progression (Sherr, 1995). We showed that the antiproliferative effect of LB42908 correlates with G_1 arrest of HUVECs stimulated with VEGF. Furthermore, our data revealed that LB42908 inhibited VEGF-induced expression of cyclins, particularly cyclin D1, and Rb phosphorylation. It indicates that LB42908 can suppress the proliferation of VEGF-stimulated endothelial cells by inhibiting the cyclin D1 expression and Rb phosphorylation. On the other hand, the cell-cycle checkpoint G_1 arrest is also mediated by up-regulating the CDK inhibitors p21 and p27 (Sherr, 1995; Foijer and te Riele, 2006). Regulation of p21 is multifactorial, and the transcription factor p53 is one of the major upstream regulators of p21 (el-Deiry et al., 1994). Akt can also participate in the decrease of p53 protein levels via Mdm2 phosphorylation and suppress p21 expression (Sheikh et al., 1994; Shankar et al., 2008). In addition, the PI3K/Akt and MEK/ERK pathways can promote cell cycle progression through the up-regulation of cyclin D1 expression (Muise-Helmericks et al., 1998; Jirmanova et al., 2002) and direct inhibition of p27 protein levels (Collado et al., 2000; Li et al., 2009). Consistent with these studies, our data showed that LB42908 increased the protein levels of p53, p21, and p27 through the suppression of VEGF-induced Akt and ERK activation. We also found that Ras knockdown revealed inhibitory effects on cell cycle progression and protein levels of these cell cycle regulators similar to those of LB42908, indicating that Ras is an important mediator for regulating VEGF-induced cell cycle progression. These results suggest that the antiangiogenic effect of LB42908 is correlated with the down-regulation of cyclin D1 expression, CDK4-mediated Rb phosphorylation, and expression levels of cell cycle inhibitor proteins, whose events are coordinately controlled by the activation of both MEK/ERK and PI3K/Akt pathways in endothelial cells by VEGF (Fig. 7).

We further demonstrate the potential effects of LB42708 on tumor growth and angiogenesis in two xenograft tumor models of K-*Ras*-mutated HCT116 cells and wild-type Caco-2 cells. Tumor suppressive activity of LB42708 was significantly higher in K-*Ras*-mutated tumor than its wild-type tumor, and its antitumor activity was highly correlated with an inhibitory effect on tumor angiogenesis in both tumors, indicating that LB42708 can inhibit the growth of both *Ras*-mutated and wild type tumors via the suppression of tumor angiogenesis.

In conclusion, our present data suggest that the antitumor effect of LB42908 is associated with multiple mechanisms, including direct inhibition of tumor cell proliferation and survival as shown in previous studies (Lubet et al., 2006; Agrawal and Somani, 2009), the inhibition of VEGF expression (Rak et al., 2000; Han et al., 2005), and suppression of tumor angiogenesis by blocking signal transduction pathways of VEGF produced from both *Ras*-mutated and wild-type tumors.

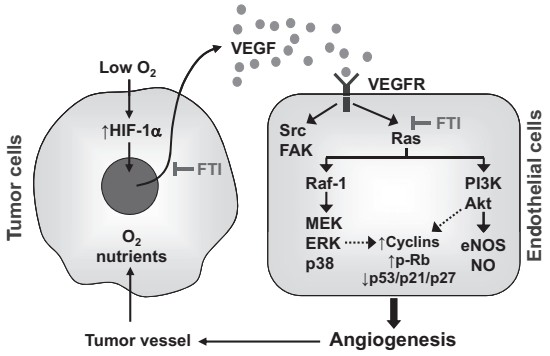

Fig. 7. The possible regulatory mechanism by which LB42708 inhibits VEGF-induced angiogenesis and signal pathways in tumor-associated endothelial cells. VEGF produced by tumors under low-oxygen condition activates its receptor KDR/Flk-1 in tumor-associated endothelial cells and elicits the Ras-dependent angiogenic signaling pathways such as Raf-1/MEK/ERK/p38 MAPK and PI3K/Akt/eNOS. Both pathways may be coordinately involved in the control of cell cycle progression by regulating the expression of cyclins, p21, and p27, as well as controlling Rb phosphorylation. LB42708 can directly suppress VEGF production from tumor cells (Rak et al., 2000; Han et al., 2005) as well as inhibit farnesylation-mediated activation of Ras, which is downstream of VEGF receptor activation.

Acknowledgments

We thank Elaine Por for helpful comments and critical reading of this manuscript.

References

Adjei AA (2001) Blocking oncogenic Ras signaling for cancer therapy. *J Natl Cancer Inst* **93:**1062–1074.
Agrawal AG and Somani RR (2009) Farnesyltransferase inhibitor as anticancer agent. *Mini Rev Med Chem* **9:**638–652.
Collado M, Medema RH, Garcia-Cao I, Dubuisson ML, Barradas M, Glassford J, Rivas C, Burgering BM, Serrano M, and Lam EW (2000) Inhibition of the phosphoinositide 3-kinase pathway induces a senescence-like arrest mediated by p27Kip1. *J Biol Chem* **275:**21960–21968.
Des Guetz G, Uzzan B, Nicolas P, Cucherat M, Morere JF, Benamouzig R, Breau JL, and Perret GY (2006) Microvessel density and VEGF expression are prognostic factors in colorectal cancer. Meta-analysis of the literature. *Br J Cancer* **94:**1823–1832.
el-Deiry WS, Harper JW, O'Connor PM, Velculescu VE, Canman CE, Jackman J, Pietenpol JA, Burrell M, Hill DE, and Wang Y (1994) WAF1/CIP1 is induced in p53-mediated G1 arrest and apoptosis. *Cancer Res* **54:**1169–1174.
Ferrara N (2002) VEGF and the quest for tumour angiogenesis factors. *Nat Rev Cancer* **2:**795–803.
Foijer F and te Riele H (2006) Check, double check: the G2 barrier to cancer. *Cell Cycle* **5:**831–836.
Folkman J and Klagsbrun M (1987) Angiogenic factors. *Science* **235:**442–447.
Greenberg JI and Cheresh DA (2009) VEGF as an inhibitor of tumor vessel maturation: implications for cancer therapy. *Expert Opin Biol Ther* **9:**1347–1356.
Gu WZ, Tahir SK, Wang YC, Zhang HC, Cherian SP, O'Connor S, Leal JA, Rosenberg SH, and Ng SC (1999) Effect of novel CAAX peptidomimetic farnesyltransferase inhibitor on angiogenesis in vitro and in vivo. *Eur J Cancer* **35:**1394–1401.
Guo D, Jia Q, Song HY, Warren RS, and Donner DB (1995) Vascular endothelial cell growth factor promotes tyrosine phosphorylation of mediators of signal transduc-

Downloaded from molpharm.aspetjournals.org by guest on December 1, 2012

tion that contain SH2 domains. Association with endothelial cell proliferation. *J Biol Chem* **270:**6729–6733.
Han JY, Oh SH, Morgillo F, Myers JN, Kim E, Hong WK, and Lee HY (2005) Hypoxia-inducible factor 1alpha and antiangiogenic activity of farnesyltransferase inhibitor SCH66336 in human aerodigestive tract cancer. *J Natl Cancer Inst* **97:**1272–1286.
Hanai J, Dhanabal M, Karumanchi SA, Albanese C, Waterman M, Chan B, Ramchandran R, Pestell R, and Sukhatme VP (2002) Endostatin causes G1 arrest of endothelial cells through inhibition of cyclin D1. *J Biol Chem* **277:**16464–16469.
Head J and Johnston SR (2004) New targets for therapy in breast cancer: farnesyltransferase inhibitors. *Breast Cancer Res* **6:**262–268.
Idbaih A, Ducray F, Sierra Del Rio M, Hoang-Xuan K, and Delattre JY (2008) Therapeutic application of noncytotoxic molecular targeted therapy in gliomas: growth factor receptors and angiogenesis inhibitors. *Oncologist* **13:**978–992.
Jirmanova L, Afanassieff M, Gobert-Gosse S, Markossian S, and Savatier P (2002) Differential contributions of ERK and PI3-kinase to the regulation of cyclin D1 expression and to the control of the G1/S transition in mouse embryonic stem cells. *Oncogene* **21:**5515–5528.
Kim HS, Kim JW, Gang J, Wen J, Koh SS, Koh JS, Chung HH, and Song SY (2006) The farnesyltransferase inhibitor, LB42708, inhibits growth and induces apoptosis irreversibly in H-ras and K-ras-transformed rat intestinal epithelial cells. *Toxicol Appl Pharmacol* **215:**317–329.
Lee H, Lee J, Lee S, Shin Y, Jung W, Kim JH, Park K, Kim K, Cho HS, Ro S, et al. (2001) A novel class of highly potent, selective, and non-peptidic inhibitor of Ras farnesyltransferase (FTase). *Bioorg Med Chem Lett* **11:**3069–3072.
Lee SJ, Namkoong S, Kim YM, Kim CK, Lee H, Ha KS, Chung HT, Kwon YG, and Kim YM (2006) Fractalkine stimulates angiogenesis by activating the Raf-1/MEK/ERK- and PI3K/Akt/eNOS-dependent signal pathways. *Am J Physiol Heart Circ Physiol* **291:**H2836–H2846.
Li N, Wang C, Wu Y, Liu X, and Cao X (2009) Ca(2+)/calmodulin-dependent protein kinase II promotes cell cycle progression by directly activating MEK1 and subsequently modulating p27 phosphorylation. *J Biol Chem* **284:**3021–3027.
Liu M, Bryant MS, Chen J, Lee S, Yaremko B, Lipari P, Malkowski M, Ferrari E, Nielsen L, Prioli N, et al. (1998) Antitumor activity of SCH 66336, an orally bioavailable tricyclic inhibitor of farnesyl protein transferase, in human tumor xenograft models and wap-ras transgenic mice. *Cancer Res* **58:**4947–4956.
Lubet RA, Christov K, You M, Yao R, Steele VE, End DW, Juliana MM, and Grubbs CJ (2006) Effects of the farnesyl transferase inhibitor R115777 (Zarnestra) on mammary carcinogenesis: prevention, therapy, and role of HaRas mutations. *Mol Cancer Ther* **5:**1073–1078.
Min JK, Han KY, Kim EC, Kim YM, Lee SW, Kim OH, Kim KW, Gho YS, and Kwon YG (2004) Capsaicin inhibits in vitro and in vivo angiogenesis. *Cancer Res* **64:**644–651.
Muise-Helmericks RC, Grimes HL, Bellacosa A, Malstrom SE, Tsichlis PN, and Rosen N (1998) Cyclin D expression is controlled post-transcriptionally via a phosphatidylinositol 3-kinase/Akt-dependent pathway. *J Biol Chem* **273:**29864–29872.
Na HJ, Lee SJ, Kang YC, Cho YL, Nam WD, Kim PK, Ha KS, Chung HT, Lee H, Kwon YG, et al. (2004) Inhibition of farnesyltransferase prevents collagen-induced arthritis by down-regulation of inflammatory gene expression through suppression of p21(ras)-dependent NF-kappaB activation. *J Immunol* **173:**1276–1283.
Namkoong S, Chung BH, Ha KS, Lee H, Kwon YG, and Kim YM (2008) Microscopic technique for the detection of nitric oxide-dependent angiogenesis in an animal model. *Methods Enzymol* **441:**393–402.
Namkoong S, Lee SJ, Kim CK, Kim YM, Chung HT, Lee H, Han JA, Ha KS, Kwon YG, and Kim YM (2005) Prostaglandin E2 stimulates angiogenesis by activating the nitric oxide/cGMP pathway in human umbilical vein endothelial cells. *Exp Mol Med* **37:**588–600.
Pruitt K and Der CJ (2001) Ras and Rho regulation of the cell cycle and oncogenesis. *Cancer Lett* **171:**1–10.
Rak J, Yu JL, Klement G, and Kerbel RS (2000) Oncogenes and angiogenesis: signaling three-dimensional tumor growth. *J Investig Dermatol Symp Proc* **5:**24–33.
Ravoet C, Mineur P, Robin V, Debusscher L, Bosly A, André M, El Housni H, Soree A, Bron D, and Martiat P (2008) Farnesyl transferase inhibitor (lonafarnib) in patients with myelodysplastic syndrome or secondary acute myeloid leukaemia: a phase II study. *Ann Hematol* **87:**881–885.
Rodenhuis S (1992) Ras and human tumors. *Semin Cancer Biol* **3:**241–247.
Schubbert S, Shannon K, and Bollag G (2007) Hyperactive Ras in developmental disorders and cancer. *Nat Rev Cancer* **7:**295–308.
Scott AN, Hetheridge C, Reynolds AR, Nayak V, Hodivala-Dilke K, and Mellor H (2008) Farnesyltransferase inhibitors target multiple endothelial cell functions in angiogenesis. *Angiogenesis* **11:**337–346.
Serban D, Leng J, and Cheresh D (2008) H-ras regulates angiogenesis and vascular permeability by activation of distinct downstream effectors. *Circ Res* **102:**1350–1358.
Shankar E, Sivaprasad U, and Basu A (2008) Protein kinase C epsilon confers resistance of MCF-7 cells to TRAIL by Akt-dependent activation of Hdm2 and downregulation of p53. *Oncogene* **27:**3957–3966.
Sheikh MS, Li XS, Chen JC, Shao ZM, Ordonez JV, and Fontana JA (1994) Mechanisms of regulation of WAF1/Cip1 gene expression in human breast carcinoma: role of p53-dependent and independent signal transduction pathways. *Oncogene* **9:**3407–3415.
Sherr CJ (1995) D-type cyclins. *Trends Biochem Sci* **20:**187–190.
Zachary I (2003) VEGF signalling: integration and multi-tasking in endothelial cell biology. *Biochem Soc Trans* **31:**1171–1177.

Address correspondence to: Dr. Young-Myeong Kim, Department of Molecular and Cellular Biochemistry, School of Medicine, Kangwon National University, Chuncheon, Kangwon-do 200-701, South Korea. E-mail: ymkim@kangwon.ac.kr

MOL PHARM
MOLECULAR PHARMACOLOGY
aspet
Downloaded from molpharm.aspetjournals.org by guest on December 1, 2012